JOURNAL OF APPLIED ELECTROCHEMISTRY 23 (1993) 715–727

# Optimal time-varying potential control

R. BAKSHI, P. S. FEDKIW*

*Department of Chemical Engineering, North Carolina State University, Raleigh, NC 27695-7905, USA*

Received 26 May 1992; revised 10 September 1992

As an illustration of the potential utility of optimal-control theory, we determine the time-varying electrode potential which maximizes the desired product produced from a coupled, chemical–electrochemical reaction sequence occurring in a well-mixed batch reactor for a specified reaction time. The reactant is electrochemically reduced to a stable intermediate which is itself a reactant for two competing parallel reactions: a homogeneous chemical decomposition to the desired product, or a further electrochemical reduction to an undesired product. If the transfer coefficient of the first reaction is greater than that of the second, then chattering control, in which the potential switches at an infinite frequency between two limits, is optimal. If the transfer coefficients have the opposite relationship, then a continuous, time-varying potential is optimal. We compare the results of applying the optimal, chattering-potential control with those resulting from the best continuous and steady controls. Improved selectivity results from a chattering control and may be effected even in the presence of significant mass-transfer resistance. Since an infinite-frequency control cannot be actually implemented, we discuss how a high-frequency, rectangular waveform can be determined which results in essentially the same product distribution as a chattering control. A qualitative, simple-to-apply method to determine whether selectivity enhancement is attainable using chattering controls is also illustrated.

## Nomenclature

| | |
|---|---|
| $a$ | electrode surface area per unit volume of the reactor, $cm^{-1}$ |
| $c_i$ | bulk concentration of species $i$, $mol\,cm^{-3}$ |
| $c_{is}$ | concentration of species $i$ at the electrode surface, $mol\,cm^{-3}$ |
| $c_i^0$ | initial concentration of species $i$, $mol\,cm^{-3}$ |
| $E$ | electrode potential, V |
| $E_{c,max}$ | maximum cathodic potential, V |
| $F$ | Faraday constant, $96\,487\,C\,mol^{-1}$ |
| $f$ | $F/RT$, $V^{-1}$ |
| $J$ | functional to be maximized |
| $k_1$ | heterogeneous rate constant for reaction leading to the formation of intermediate I, $cm\,h^{-1}$ |
| $k_2$ | heterogeneous rate constant for the electrochemical decomposition of intermediate I, $cm\,h^{-1}$ |
| $k_3$ | homogeneous rate constant for the chemical decomposition of intermediate I, $h^{-1}$ |
| $k_1^*$ | $ak_1t_f$ |
| $k_2^*$ | $ak_2t_f$ |
| $k_3^*$ | $k_1t_f$ |
| $k_{mi}$ | mass-transfer coefficient of species $i$, $cm\,h^{-1}$ |
| $P_\Omega$ | projection onto the set of admissible controls |
| $r_{AI}$ | consumption rate of A in the electrochemical reaction A → I, $mol\,cm^{-2}\,h^{-1}$ |
| $r_{IU}$ | production rate of A in the electrochemical reaction I → U, $mol\,cm^{-2}\,h^{-1}$ |
| $R$ | universal gas constant, $8.314\,J\,mol^{-1}\,K^{-1}$ |
| $T$ | reaction temperature, K |
| $t$ | time, h |
| $t_f$ | batch reaction time, h |
| $t^*$ | dimensionless time, $t/t_f$ |
| $u(t)$ | control vector profile |
| $\hat{u}(t)$ | optimal-control profile |
| $u_{max}$ | maximum value of the control |
| $u_{min}$ | minimum value of the control |
| $u_{ir}$ | control $i$ in the relaxed set |
| $x$ | vector of state variables |
| $x_i$ | dimensionless concentration of species $i$, $c_i/c_A^0$ |

*Greek symbols*

| | |
|---|---|
| $\alpha_1$ | transfer coefficient of desired cathodic reaction |
| $\alpha_2$ | transfer coefficient of undesired cathodic reaction |
| $\delta$ | thickness of the Nernst film, cm |
| $\theta^k$ | fraction of an infinitesimal time the control is held at $u^k$, duty cycle |
| $\sigma$ | step length in the direction of increasing $J$ |
| $\Omega$ | Hilbert space of admissible controls |
| $\Omega_r$ | Hilbert space of relaxed controls |

## 1. Introduction

In a globally competitive chemical industry, emphasis must be placed on the mode of operation of chemical

* Author to whom all correspondence should be addressed

0021-891X 

reactors, the heart of the process. It is therefore logical to strive for an increase in reactant conversion to the desired product while minimizing undesired reactions. A proper choice of process variables may enhance reaction selectivity; for example, Sakellaropoulous [1] discussed the effect of electrode potential, concentration, and mixing on the selectivity of certain reaction networks, and Sakellaropoulous and Francis [2] studied the effect of diffusion on selectivity within porous electrodes. In addition to the judicious choice for steady (static) settings for the process variables, selectivity may also be enhanced by optimal time-varying (dynamic) control. Optimal-control theory was introduced 25 years ago to calculate dynamic temperature-control strategies for chemical reactors to enhance reaction selectivity [3–5], but it has not been extensively applied to electrochemical reactors (e.g. [6,7]), although static optimization of electrochemical processes is a well discussed topic. In contrast to chemical reactors, the dynamic manipulation of voltage or current is much easier than temperature (or concentration, flowrate, pressure etc.) and offers intriguing possibilities for reaction engineering. Due to the typically large thermal inertia of reactors, rapid temperature variations cannot be implemented. Likewise, rapid changes in the bulk concentration are attenuated by mass-transfer resistance and, in heterogeneous reactors, cannot significantly affect the concentration at the surface, the site of the reaction. In contrast, it is possible to use control strategies in which the potential or current is rapidly perturbed since the electrical 'inertial' effect (double-layer charging/discharging) although present, is considerably diminished in magnitude in comparison to thermal or mass-transfer inertia. Actually, electroplaters routinely employ pulse plating (e.g. [8–11]); thus nonsteady control is currently practiced, although with *a priori* choice of the control waveform.

A goal of this paper is to illustrate the utility of optimal-control theory and potential benefits realized upon its application. As a vehicle to do so, we determine the optimal time-varying electrode potential that maximizes the production of the desired product D in a batch reactor for the E–C, E reaction shown in Fig. 1, a scheme similar to that for the reduction of nitrobenzene (A) to the desired product *p*-aminophenol (D) and the undesired product aniline (U) through the intermediate phenylhydroxylamine (I) [12]. We emphasize that the particular chemistry examined is of secondary importance in comparison to the illustration of optimal-control concepts applied to an electrochemical reactor. We will demonstrate that the optimal control of electrode potential may lead to a substantial improvement in reactor performance over the best steady value.

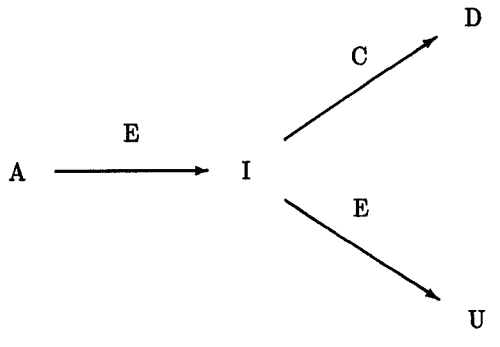


Fig. 1. Depiction of the E–C, E reaction scheme. The intermediate I is a stable species, and the chemical step is homogeneous.

The optimal, time-varying control of potential or current can be used to achieve objectives other than maximizing productivity; for example, the current efficiency or selectivity can be maximized, or the power consumption can be minimized. In electrodeposition the objective may be the formation of a desired alloy or spatial-composition gradients when plating from multiple-salt baths. It is our intent to provide sufficient incentive for practitioners to consider devising optimal-control strategies for their particular application and objectives.

The paper is organized as follows. We first describe the physical model of the reactor and the mathematical problem statement. This is followed by a description of the optimization method employed after which we discuss the computational results and provide a physical basis for the predicted trends. Finally, some generalizations are presented. Computational details are not presented, but are available in the dissertation upon which this work is based [13].

## 2. Model and problem statement

### 2.1. Reactor model

Simplifying assumptions are made about the transport and kinetic processes to reduce computational effort while still capturing the essential phenomena. In this manner, we focus on the improvements resulting from application of the optimal-potential control. We assume: (i) the reactor is well-mixed with mass-transfer resistance occurring by material diffusion through a Nernst diffusion layer as quantified with a mass-transfer coefficient; (ii) the homogeneous chemical reaction I $\rightarrow$ D follows first-order kinetics in the bulk and consumes an inconsequential amount of reactant in the thin Nernst layer; (iii) no other reactions in addition to those shown in Fig. 1 occur; (iv) the capacitance of the double layer is negligible; (v) the current distribution is uniform; and (vi) the charge-transfer reactions are irreversible with a Tafel-potential behaviour and a first-order dependence on reactant concentration.

### 2.2. Mathematical problem statement

The objective is to determine the time-varying electrode potential which maximizes $c_D(t_f)$, the concentration of the desired product at the end of a specified batch period $t_f$. In a more general sense, we want to determine the control $u(t)$ which maximizes the functional $J[u(t)]$, where $u(t)$ may be

potential or some function of it. For the example under consideration, the functional is

$$J[u(t)] = c_D(t_f) \tag{1}$$

Only reactant A is present at $t = 0$, which results in the initial conditions

$$c_A(0) = c_A^0 \tag{2}$$

$$c_i(0) = 0, \qquad i = I, D, U \tag{3}$$

The material-balance equations must be satisfied and, subject to the listed assumptions, may be written as

$$\dot{c}_A = -ar_{AI} = -ak_1 c_{As} e^{-\alpha_1 fE} \tag{4}$$

$$\dot{c}_I = ak_1 c_{As} e^{-\alpha_1 fE} - ak_2 c_{Is} e^{-\alpha_2 fE} - k_3 c_I \tag{5}$$

$$\dot{c}_D = k_3 c_I \tag{6}$$

$$\dot{c}_U = ar_{IU} = ak_2 c_{Is} e^{-\alpha_2 fE} \tag{7}$$

where $c_i$ is the bulk concentration of species $i$, $\dot{c}_i \equiv dc_i/dt$, $c_{is}$ is the concentration at the electrode surface which differs from the bulk because of the presence of mass-transfer resistance, $r_{AI}$ and $r_{IU}$ are the consumption rate of A and the production rate of U per unit electrode area, respectively, $k_1$ and $k_2$ are potential-independent, heterogeneous rate constants, $k_3$ is the first-order, homogeneous rate constant, $a$ is the electrode surface area per unit volume of the reactor, $E$ is the electrode potential relative to some reference electrode, and $f = F/RT$. Before the material-balance equations can be solved, the surface concentrations must be related to the bulk values, but we defer that discussion until after the optimization technique used is presented.

To restrict the number of variables to be optimized, the electrode potential is *a priori* constrained as

$$E_{c,max} \leqslant E \leqslant \infty \tag{8}$$

where the cathode bound $E_{c,max}$ may be imposed to avoid undesired electrolyte and/or solvent electrochemistry, and the anodic bound ensures zero rates of the electrochemical reductions A → I and I → U. We also assume that no anodic decomposition of the solvent occurs. Actually, a finite anodic bound could be set to assure negligible electrochemical reaction rates of A and I and solvent; however, to reduce the number of parameters, the anodic limit is set to infinity. The two potential limits could be left unspecified and also be optimized, but the associated complexity would not add to our intent of illustrating the utility of optimal-control theory.

In the remainder of Section 2, we discuss the application of optimal-control theory to the problem at hand. A reader not (yet) interested in these details might first skip to the Results and Discussion Section to gain an appreciation of the benefits to be gained upon its application.

### 2.3. *Dynamic optimization procedures*

The theory of optimal control is discussed in a number of textbooks (e.g. [14–17]), and optimal controls can be determined using a variety of techniques, for example: (i) application of variational calculus in which the optimal control is found as a solution to a system of coupled differential and algebraic equations (e.g. [4, 5, 18, 19]); (ii) use of Pontryagin's maximum principle in which the control is chosen to maximize the Hamiltonian of the system (e.g. [20]); (iii) control-vector parameterization in which the control $u(t)$ is written in terms of unknown parameters $a_j$ and postulated functions $\psi_j(t)$ as $u(t) = \sum_{j=1}^{n} a_j \psi_j(t)$, and the $a_j$ are determined by nonlinear programming procedures to maximize the objective functional (e.g. [14, 21–24]); or (iv) control-vector iteration in which a gradient-search in the space of the controls is applied to maximize $J$ (e.g. [25–27]). The first procedure is useful when the control is unconstrained; the second is an elegant mathematical relationship and is useful when the Hamiltonian of the system is linear in the control; and the third, while in many cases computationally efficient, limits the form of the control through the *a priori* chosen $\psi_j(t)$. Control-vector iteration is used here because of the ease with which control constraints can be taken into account and the relatively straight-forward manner in which the calculations proceed.

Before the control-vector iteration technique is discussed, it is first advantageous to introduce two new control variables $u_1(t)$ and $u_2(t)$ defined in terms of the potential as

$$u_1(t) = e^{-\alpha_1 fE(t)} \tag{9}$$

$$u_2(t) = e^{-\alpha_2 fE(t)} \tag{10}$$

with the two related by

$$u_1 = u_2^{\alpha_1/\alpha_2} \tag{11}$$

and, because of the constraints on the potential, are bounded as

$$0 \leqslant u_1 \leqslant u_{1\,max} \qquad u_{1\,max} = e^{-\alpha_1 fE_{e,max}} \tag{12}$$

$$0 \leqslant u_2 \leqslant u_{2\,max} \qquad u_{2\,max} = e^{-\alpha_2 fE_{e,max}} \tag{13}$$

We shall calculate the optimal-potential profile $E(t)$ by actually searching for the two optimal $u_i(t)$. The motivation for introducing $u_1(t)$ and $u_2(t)$ is certainly not transparent at this point. However, we will show: (1) that the relationship between the two (Equation 11) provides a geometric framework about which the optimal potential $E(t)$ is determined (Section 2.3.1); (2) that the class of controls from which the optimal is searched is enlarged by the introduction of $u(t)$ (Section 2.3.3); and (3) that a simple qualitative examination of the controls in this formulation can be performed to determine if the optimal-potential control is of a certain type (Section 3.2). These advantages outweigh the seeming complexity of introducing in the analysis two related controls to replace one.

The material-balance equations in terms of $u$ are rewritten as

$$\dot{c}_A = -ak_1 c_{As} u_1 \tag{14}$$

$$\dot{c}_I = ak_1 c_{As} u_1 - ak_2 c_{Is} u_2 - k_3 c_I \tag{15}$$

$$\dot{c}_D = k_3 c_I \tag{16}$$

$$\dot{c}_U = ak_2 c_{Is} u_2 \tag{17}$$

In a dimensionless form, the vector set of the above equations, after elimination of the surface concentrations, can be succinctly written as

$$\dot{x} = f(x, u) \tag{18}$$

where $x$ and $u$ are vectors representing the state (dimensionless concentrations) and controls (Equations 9 and 10), respectively.

*2.3.1. Control-vector iteration*: The central idea of control-vector iteration is to find a $v(t)$ which is a perturbation in a control vector $u(t)$ such that $J$ is increased; i.e.

$$J[(u(t) + v(t)] > J[u(t)] \tag{19}$$

Once such a $v(t)$ is found, the control is improved in an iterative manner by replacing $u(t)$ by $u(t) + v(t)$ until no further increase in $J$ occurs. It can be shown that if the control is unconstrained, then Equation 19 is valid if $v(t)$ is a small perturbation in the direction of $\nabla J[u(t)]$ where $\nabla J[u(t)]$ is the gradient of the functional in the Hilbert space of controls [28]. Hence, the following iterative gradient-search scheme may be used to find the optimal control $\hat{u}(t)$

$$u^{(i+1)}(t) = u^{(i)}(t) + \sigma^{(i)} \nabla J[u^{(i)}(t)] \tag{20}$$

where the scalar step-length $\sigma^{(i)}$ may be varied at each iteration $i$ to hasten convergence, e.g. the Armijo step-length rule [29] may be applied. In application of Equation 20, the gradient $\nabla J[u(t)]$ is calculated by [25, 28]

$$\nabla J[u(t)] = \nabla H[u(t)] \tag{21}$$

where $\nabla H[u(t)]$ is the gradient of the Hamiltonian $H$ with components $\partial H/\partial u_i$. For the dynamic system described by Equation 18 with a functional of the form given in Equation 1, the Hamiltonian $H$ is

$$H = p^T(t) f(x(t), u(t)) \tag{22}$$

where $p(t)$ denotes the adjoint vector with elements $p_i(t)$ obtained by solving the adjoint equations

$$\dot{p}_i = -\frac{\partial H}{\partial x_i} \qquad p_i(t_f) = \left.\frac{\partial J}{\partial x_i}\right|_{x(t_f)} \tag{23}$$

The five-step procedure to determine the optimal control $\hat{u}(t)$ can now be outlined: (i) Guess an initial control vector $u^{(i)}(t)$; (ii) Solve numerically the material-balance equations; (iii) Solve numerically the adjoint equations; (iv) Calculate the gradient of the functional (Equation 21); and (v) Calculate the new control vector $u^{(i+1)}(t)$ from Equation 20. Steps 2 to 5 are repeated until the functional $J$, calculated after step 2, has changed by less than $10^{-3}$%.

In many problems, the controls are constrained to lie within a specified region $\Omega$ of the Hilbert space of controls and are called 'admissible controls'. In the example under consideration, the admissible controls are on line segment OCP in Fig. 2 and are specified by the bounds on $u_i$ and Equation 11. In the presence of control constraints, Equation 20 cannot be applied as written since it may predict a control $u^{(i+1)}(t)$ that lies outside the permissible region. However, if $\Omega$ is a convex set*, then the gradient-projection method can be employed to find the optimal control $\hat{u}(t)$ in an iterative manner as [25–27, 30]

$$u^{(i+1)}(t) = P_\Omega\{u^{(i)}(t) + \sigma^{(i)} \nabla J[u^{(i)}(t)]\} \tag{24}$$

where $P_\Omega\{\cdot\}$ signifies the projection of $u^{(i)}(t) + \sigma^{(i)} \nabla J[u^{(i)}(t)]$ on to $\Omega$ and is an identity operator for any control that lies in $\Omega$. Note that in the latter case Equations 24 and 20 are identical. Algorithms can be implemented to hasten the convergence of Equation 24 by choosing an appropriate value for

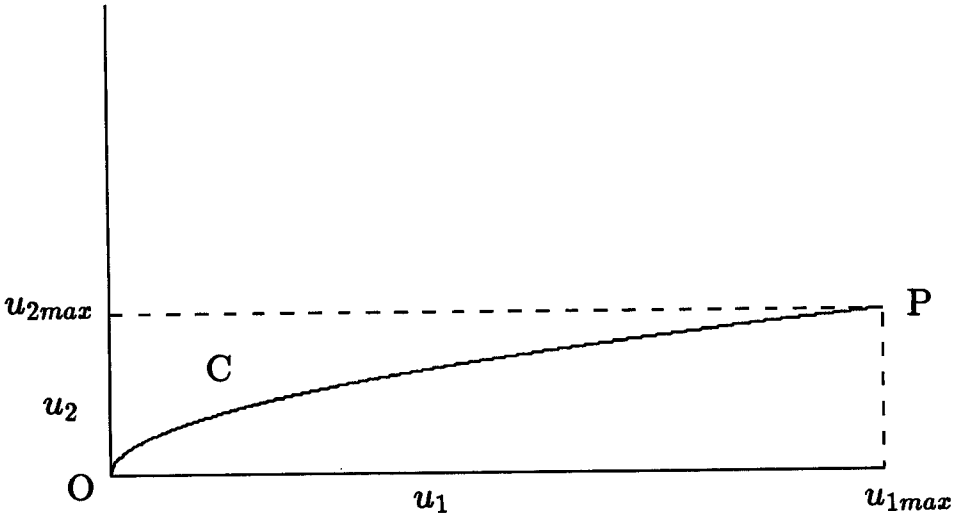


Fig. 2. Line segment OCP is the set of admissible controls described by Equations 8 and 11 with $\alpha_1 > \alpha_2$.

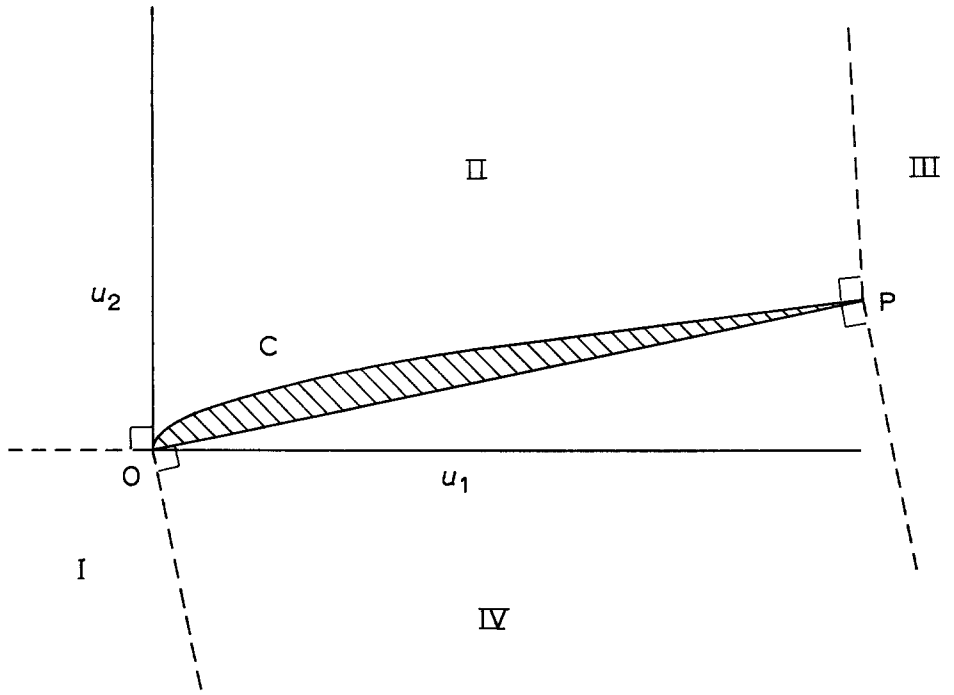


Fig. 3. The relaxed set of controls $\Omega_r$ is depicted by the shaded region and is the convex hull of the admissible set $\Omega$, line segment OCP. The relaxed set forms the control space over which the gradient-projection method is applied. The dotted lines demarcate regions I, II, III, and IV from which, during the application of Equation 24, the controls are projected onto point O, segment OCP, point P, and segment OP, respectively.

the step-length $\sigma^{(i)}$ [26]; for example, we choose the Bertsekas step-length rule [13, 31]. The five-step calculation scheme outlined in the previous paragraph to determine the optimal control $\hat{u}(t)$ is slightly modified for constrained controls: If the predicted control $u^{(i+1)}(t)$ in step 5 is not in $\Omega$, then the projection operation is carried out before returning to step 2.

The control space of the example problem is nonconvex (Fig. 2), and the gradient-projection method cannot be applied; however, if the convex hull† of $\Omega$ is formed, as shown on Fig. 3 and designated as the relaxed set $\Omega_r$, the gradient-projection method may then be applied to $\Omega_r$ to calculate the optimal control $\hat{u}_r(t)$. Since only controls which lie on OCP are physically realizable, the question must be addressed how does one actually establish a control for any $u_r(t) \in \Omega_r$ where $u_r(t) \notin \Omega$. The literature discussed in the following section demonstrates that reaction velocities $\dot{x}$ generated by any such $u_r(t)$ for the example problem can be obtained by rapidly switching (i.e. at an infinite frequency) the controls from physically realizable $u(t) \in \Omega$. The descriptive term applied to this control type is 'chattering control'. Hence, a chattering control using admissible $u(t)$ is the manner to generate a relaxed control $u_r(t)$.

*2.3.2. Chattering potential control*: It has been shown (e.g. [32–34]) that when a control $u$ switches between $m$ admissible values $(u^1 \ldots u^k \ldots u^m)$ over an infinitesimal time $\delta t \to 0$ such that the control is held at $u^k$ for a fraction $\theta^k$ of $\delta t$ (i.e. a chattering control), the reaction velocity $\dot{x}$ for the system described by Equation 18 can be written as

$$\dot{x} = \sum_{k=1}^{m} \theta^k f(x, u^k) \tag{25}$$

Fjeld [33] and Gamkrelidze [34] have explained the concept of chattering control using probability theory: $\theta^k$ is interpreted as the probability that the control at any instant is $u^k$. Therefore, for a chattering control resulting in a reaction velocity $\dot{x}$ which is equal to that generated by a relaxed control $u_r(t)$, we can write

$$\dot{x} = f(x, u_r) = \sum_{k=1}^{m} \theta^k f(x, u^k) \tag{26}$$

where $m$, $\theta^k$, and $u^k$ are to be determined, with an upper bound on $m$ being the dimension of the vector $f$ [32–34].

To proceed further we first consider the mass-transfer conditions which would exist under a chattering potential control. The potential is switched between limit values so quickly that transient mass-transfer effects cannot occur; that is, the surface concentration of the reactants and products cannot adjust to the rapidly varying potential. It is impossible to apply a potential for an infinitesimal time, but it is possible to set the potential at each limit for a time that is sufficiently small such that surface concentrations do not vary significantly during it. To clarify this

* A set is convex if a weighted linear combination of any two elements of the set also lies in the set, with the weight factors being positive, less than one, and summing to unity.

† The convex hull of a set is the smallest convex set which encloses it.

concept, Fig. 4 illustrates the calculated concentration behaviour for a 'real system'. The concentrations of nitrobenzene (A) and phenylhydroxylamine (I) at the cathode surface of a parallel-plate reactor calculated by solving the transient-diffusion equation in a Nernst layer are shown when the cell voltage is a periodic square wave [35]. The high-frequency behaviour shows that the surface concentration obtains a nearly steady value, a so-called 'relaxed state'. Therefore, when the potential rapidly switches over the infinitesimal interval $\delta t$ between $m$ admissible $E^k$ with corresponding $u_i^k = \exp[-\alpha_i f E^k]$, the reaction rates $r_{AI}$ and $r_{IU}$ (Equations 14 and 17) may be written as

$$r_{AI} = k_1 c_{As} \sum_{k=1}^{m} \theta^k u_1^k \tag{27}$$

$$r_{IU} = k_2 c_{Is} \sum_{k=1}^{m} \theta^k u_2^k \tag{28}$$

since the surface concentrations of A and I remain constant over $\delta t$.

If the $i$th component of the average value of the chattering control (i.e. $\Sigma\theta^k u_i^k$) is set equal to the corresponding component of the relaxed control (i.e. $u_{ri}$), the resulting reaction velocities in the state equations are identical to those obtained from applying the relaxed control; that is Equation 26 is satisfied by

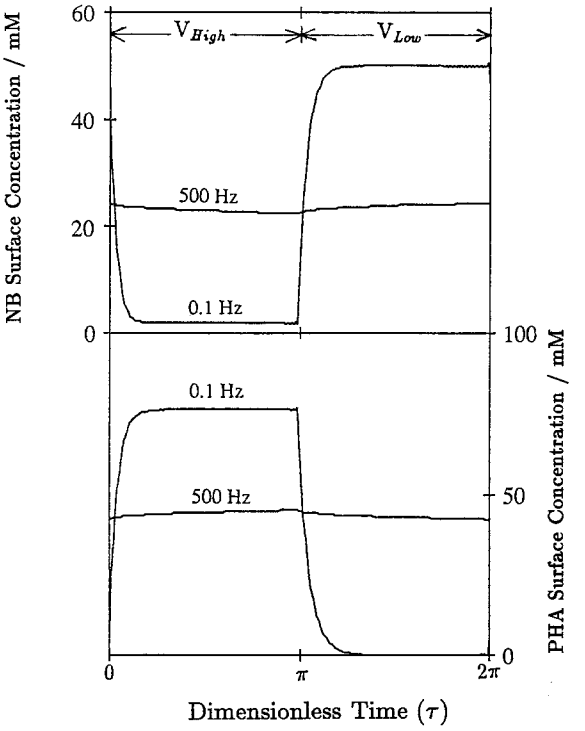


Fig. 4. The concentrations of nitrobenzene (NB) and phenylhydroxylamine (PHA) at the cathode surface of a parallel-plate reactor over one dimensionless cycle when the cell voltage is a square wave switching between the two voltages $V_{high}$ and $V_{low}$ at 500 and 0.1 Hz [32]. The solution to the transient-diffusion equation within the Nernst layers was used to generate these results which illustrate that at high-frequency oscillation the surface concentration obtains a steady, so-called 'relaxed', value.

writing

$$u_r(t) = \sum_{k=1}^{m} \theta^k u^k$$
$$\sum_{k=1}^{m} \theta^k = 1 \qquad 0 \leqslant \theta^k \leqslant 1 \tag{29}$$

where $u^k$ is a vector $(u_1, u_2)^T$ in $\Omega$ (i.e. on segment OCP in Fig. 3) and $\theta^k$ and $u^k$ may both, in general, be functions of time. Because $\Omega_r$ for the example problem is two dimensional and convex, every $u_r(t) \in \Omega_r$ can be obtained by a linear combination of two controls on segment OCP, i.e. $m = 2$. This is an application of a known property of connected convex sets which states that any point $u$ in an $n$ dimensional set can be obtained by a linear combination of $n$ points $u^j$ from the set [36], and is easily seen on Fig. 3 since a straight line can be drawn between any two points on OCP to intersect a $u_r(t)$ in the shaded region. Hence, we can write

$$u_r(t) = \theta(t)u^1(t) + (1 - \theta(t))u^2(t) \tag{30}$$

From knowledge of the coordinates of the optimal $\hat{u}_r(t)$ obtained by application of the gradient-projection method, $\theta(t)$, $u^1(t)$, and $u^2(t)$ may now be determined.

*2.3.3. Rectangular waveform as approximation to a chattering control*: On applying the gradient-projection method to the example problem, the optimal relaxed control $\hat{u}_r(t)$ was calculated to lie on segment OP if $\alpha_1 > \alpha_2$. Therefore, the optimal control is a chattering control which switches between the two admissible values $P(u = u_{max})$ and $O(u = u_{min})$, and Equation 30 becomes

$$u_r(t) = \theta(t)u_{max} + [1 - \theta(t)]u_{min} \tag{31}$$

where the weight factor $\theta(t)$ is the instantaneous duty cycle, i.e. the probability at any instant that the control is at $u_{max}$. Equation 31 can be rearranged to solve for the $\theta(t)$ which yields an average value of the chattering control equal to the optimal relaxed control $\hat{u}_r(t)$ as

$$\theta(t) = \frac{\hat{u}_r(t)}{u_{max}} \tag{32}$$

since $u_{min} = 0$.

Clearly, it is impossible to switch the potential between the two limits at an infinite rate. However, there will typically exist a small, finite time for which if the potential is held for this duration transient mass-transfer effects do not occur to a significant extent, yet it is sufficiently large such that double-layer charge accounts for only a small fraction of the coulombs passed during it. (In a subsequent communication [37], we quantify this timespan in the course of discussing chattering cell-voltage control for a parallel-plate reactor. Puippe and Ibl [38] have addressed

similar considerations for the effect of capacitance in pulsed-current plating.) In other words, a high-frequency, rectangular-potential waveform will lead to a state profile which closely approximates that which would be obtained from a chattering control. The fraction of the cycle time $\Theta$ for which the potential is maintained at the cathodic limit $E_{c,\max}$ in the rectangular-waveform approximation is determined by use of Equation 32 which indicates that the duty cycle $\theta(t)$ of the chattering control varies continuously; but in applying a rectangular-potential profile, its duty cycle can only be varied discretely. These discrete values can be calculated by dividing the batch period into small, equally-spaced intervals $\Delta t$ equal to the period of the high-frequency rectangular waveform ($\Delta t \ll t_f$) and approximating the continuous profile $\theta(t)$ with a duty cycle $\Theta_i$ of a rectangular waveform over an $i$th interval as

$$\Theta_i = \frac{1}{\Delta t}\int_{t_{i-1}}^{t_i} \theta(t)\mathrm{d}t \tag{33}$$

The motivation for introducing the controls $u_1(t)$ and $u_2(t)$ can now be stated. In the relaxed control space $\Omega_r$, the gradient-projection method searches for an optimal control from a class which is larger than continuous or piecewise-continuous controls, i.e. the search also includes chattering controls. If the alternative approach of considering the potential $E(t)$ as the control were adopted, the control space is certainly convex and the gradient-projection method could be applied directly; it would lead, however, only to continuous or piecewise-continuous controls. In contrast, the procedure we have outlined shows unequivocally that chattering control is optimal for the example problem if $\alpha_1 > \alpha_2$, although its practical implementation is through a high-frequency, rectangular (i.e. piecewise-continuous) control.

*2.3.4. Continuous potential control*: The above development demonstrates how the optimal-potential control may be calculated. It is also reasonable to examine the best, not necessarily optimal, control if the class of controls is restricted. In this vein, we have also studied and report upon the results if the control is *a priori* specified to be continuous and in the admissible control space $\Omega$, i.e. the potential is continuous and satisfies Equation 8. Actually, as later discussed, if $\alpha_2 > \alpha_1$, the optimal control is continuous.

We calculate the best continuous potential control by replacing $u_1$ by $u_2^{\alpha_1/\alpha_2}$ in Equation 18, an approach equivalent to using $E(t)$ as the control. The dimension of the control space is thereby reduced by one to a straight line $0 \leqslant u_2 \leqslant \exp[-\alpha_2 f E_{c,\max}]$ which is a convex set and the gradient-projection method can then be used to determine $\hat{u}_2(t)$. We start the gradient-projection iteration scheme with a continuous $u_2(t)$ profile calculated from a guessed continuous $E(t)$. Since $\nabla J[u(t)]$ is continuous given a continuous $u(t)$, subsequent iterations lead to control profiles which are likewise, provided $f_u(x,u)$ exist and are continuous [28] which is true for the example examined here.

### *2.4. Elimination of surface concentrations from the state equations*

Before the controls can be calculated from the methods discussed above, the surface concentrations must be eliminated from the state equations. We accomplish this by applying a mass balance across the Nernst diffusion layer. In the following, the controls are written as $u_1$ and $u_2$ and assumed to be continuous; however, the resultant effect of a chattering control, as seen by Equations 27–29, is equivalent to a continuous relaxed control and the results presented below (Equations 38–41) are also applicable with $u_i$ replaced by $u_{ir}$.

For reactant A a material balance across the diffusion layer yields

$$k_{mA}(c_A - c_{As}) = r_{AI} = k_1 c_{As} u_1 \tag{34}$$

where $k_{mA}$ is the mass-transfer coefficient of species A. Transient concentration changes which occur when the potential varies are not accounted for in Equation 34. However, these can be neglected when the change in controls is small over the characteristic diffusion time $t_D(\delta^2/D)$. Equation 34 is rearranged to relate the surface to the bulk concentration as

$$c_{As} = \frac{k_{mA} c_A}{k_1 u_1 + k_{mA}} \tag{35}$$

Similarly, assuming the amount of intermediate I which reacts within the Nernst layer is negligible, i.e. $k_3\delta/k_{mI} \ll 1$, a material balance yields

$$k_{mI}(c_I - c_{Is}) = r_{IU} - r_{AI} = k_2 c_{Is} u_2 - k_1 c_{As} u_1 \tag{36}$$

where $k_{mI}$ is the mass-transfer coefficient of species I. Rearranging Equation 36 and using Equation 35 yields

$$c_{Is} = \frac{1}{k_2 u_2 + k_{mI}}\left(k_{mI} c_I + k_1 u_1 \frac{k_{mA} c_A}{k_1 u_1 + k_{mA}}\right) \tag{37}$$

Equations 14–17 can be written in dimensionless form using Equations 35 and 37 to eliminate the surface concentrations as

$$\dot{x}_A = -k_1^* x_{As} u_1 \qquad x_{As} = \frac{k_{mA} x_A}{k_1 u_1 + k_{mA}} \tag{38}$$

$$\dot{x}_I = k_1^* x_{As} u_1 - k_3^* x_I - k_2^* x_{Is} u_2 \tag{39}$$

$$\dot{x}_D = k_3^* x_I \tag{40}$$

$$\left.\begin{aligned} \dot{x}_U &= k_2^* x_{Is} u_2 \\ x_{Is} &= \frac{1}{k_2 u_2 + k_{mI}}\left(k_{mI} x_I + k_1 u_1 \frac{k_{mA} x_A}{k_1 u_1 + k_{mA}}\right) \end{aligned}\right\} \tag{41}$$

where $x_i \equiv c_i/c_A^0$ is the dimensionless bulk concentration of species $i$, $k_i^* \equiv a k_i t_f$ for $i = 1$ or 2, $k_3^* = k_3 t_f$, $\dot{x}_i \equiv \mathrm{d}x_i/\mathrm{d}t^*$ is the dimensionless reaction velocity, and $t^* \equiv t/t_f$ is the dimensionless time. The

*Table 1. Parameters used in the computations.*

| *Parameter* | *Value* |
|---|---|
| $k_1^*$ | $10^{-4}$ |
| $k_2^*$ | $10^{-2}$ |
| $k_3^*$ | 1.0 |
| $\alpha_1$ | 0.4 |
| $a_2$ | 0.2 |
| $fE_{c,\max}$ | 39.1 |

initial conditions become

$$x_A(0) = 1.0 \tag{42}$$

$$x_i(0) = 0, \qquad i = I, D, U \tag{43}$$

## 3. Results and discussion

The parameters used in the computations are reported in Table 1. It is not our intent to represent a particular chemical system; rather, we use the E–C, E reaction sequence to illustrate potential benefits of applying optimal-control theory. However, the parameters are similar (but not identical) to those for the reduction of nitrobenzene [12]. To illustrate the effect of mass-transfer resistance on the optimal-potential profile, and in the spirit of introducing the fewest number of parameters, we arbitrarily set $k_{mA} = 2k_{mI} = 4k_m$ where $k_m$ is the parameter varied in the computations from 1 to $10^5$ cm h$^{-1}$. This range corresponds to a variation from 0.002 to 200 in $k_m/k_1 u_{1\max}$, a ratio indicative of the kinetic to mass-transfer resistance, and spans a set of conditions from mass-transport to kinetic-controlled conditions.

Regardless of the value of $k_i^*$ $(i = 1,2,3)$, the optimal-potential profile was a chattering control if $\alpha_1 > \alpha_2$ and was a continuous, time-varying potential if $\alpha_2 > \alpha_1$, although the latter case is not discussed quantitatively here. The extent of the improvement in production and selectivity upon applying the optimal potential above the best steady control will, however, depend upon the values of $k_i^*$.

### 3.1. Comparison of time-varying and steady-potential control

Figures 5 and 6 are the best continuous and optimal chattering controls, respectively, calculated using the gradient-projection method with the parameter values of Table 1. Figure 7 shows the resultant concentration profiles over the batch period, including that for the best steady-potential control, in the limit of low (Fig. 7a) and high (Fig. 7b) mass-transfer resistance. (The best steady potential was found by solving numerically Equations 38–43 for potentials differing by 0.01 V from 1 to −1 V and locating that corresponding to the maximum $x_D(t_f)$. Table 2 lists the resultant dimensionless concentrations of the desired and undesired species at the end of the batch period for all three control strategies.

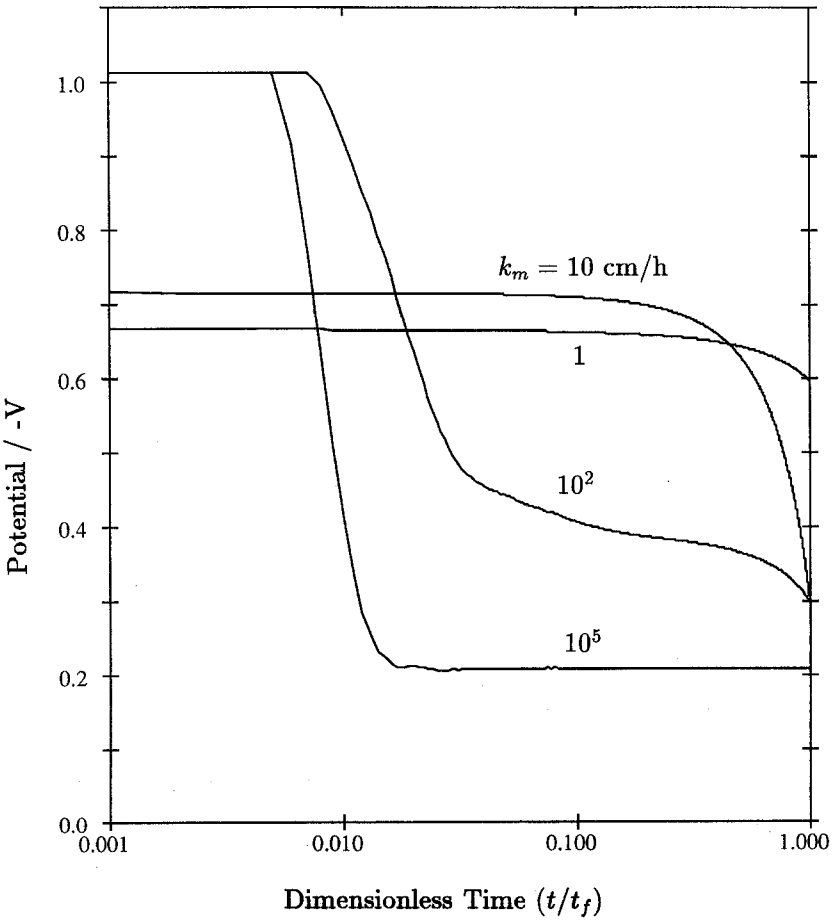


Fig. 5. The best continuous electrode potential at different mass-transfer resistances.

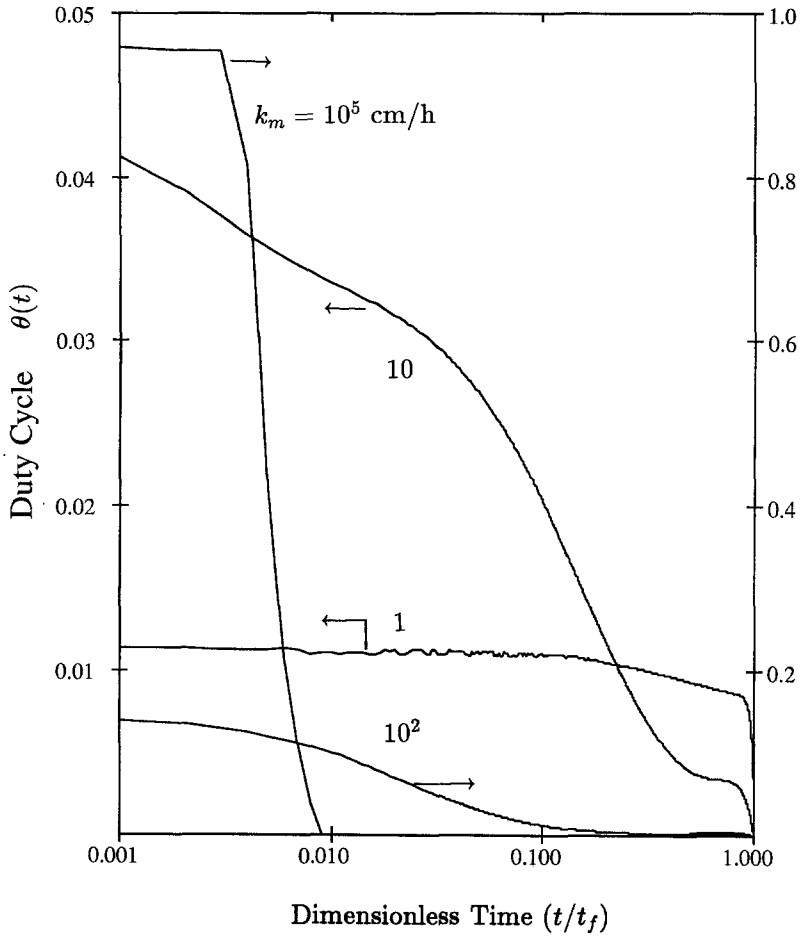


Fig. 6. The instantaneous duty cycle $\theta(t)$ for the optimal chattering potential control at various mass-transfer resistances. The potential switches between $E_{c,\max}$ and $\infty$ at effectively an infinite rate.

The greatest production of the desired compound is obtained by the optimal chattering potential control, followed in order by the best time-varying continuous and steady-potential control. The improvement provided by continuous control decreases as the mass-transfer resistance increases because of the diminished sensitivity of the reaction rates to the potential; with chattering potential control, however, the percentage increase in the production and selectivity above the steady-control value increases with decreasing $k_m$. This interesting result is caused by the small duty cycle (Fig.6) and the application of $E_{c,\max}$ during it; in this manner, mass-transfer limitations are not as significant since electrochemical reactions are not occurring for the majority of the time during $\delta t$. Of course, the production rate of the desired component D decreases for all three controls with increasing mass-transfer resistance.

*Table 2. Dimensionless concentrations of the desired and undesired products at the end of the batch period by applying the best steady, best continuous, and optimal chattering potential controls*

| $k_m/(\mathrm{cm\,h^{-1}})$ | $x_D^s$ | $x_D^{\mathrm{cont}}$ | $x_D^{\mathrm{chat}}$ |
|---|---|---|---|
| $10^5$ | 0.29 | 0.53 | 0.55 |
| $10^2$ | 0.28 | 0.41 | 0.54 |
| 10 | 0.27 | 0.27 | 0.51 |
| 1 | 0.15 | 0.15 | 0.36 |

| $k_m/(\mathrm{cm\,h^{-1}})$ | $x_U^s$ | $x_U^{\mathrm{cont}}$ | $x_U^{\mathrm{chat}}$ |
|---|---|---|---|
| $10^5$ | 0.55 | 0.14 | 0.10 |
| $10^2$ | 0.55 | 0.30 | 0.10 |
| 10 | 0.55 | 0.45 | 0.12 |
| 1 | 0.56 | 0.51 | 0.18 |

At kinetic-controlled conditions ($k_m = 10^5\,\mathrm{cm\,h^{-1}}$), the potential for continuous control (Fig. 5) and duty cycle for chattering control (Fig. 6) are largest initially which enables rapid conversion of species A to the intermediate I. After a short time, however, the potential or the duty cycle quickly decreases so that the intermediate may decompose chemically to the desired compound with little electroreduction of I to the undesired compound. Regardless of the value of $k_m$, the duty cycle and the cathodic potential for the chattering and the continuous control, respectively, decrease over the batch period to favour chemical decomposition of the intermediate to the desired product while keeping the undesired electroreduction of I to U low. In contrast, under steady-potential control it is not possible to restrict the formation of U, and its concentration continues to increase by consuming I which otherwise could have been used to form the desired product D (Fig. 7). As mass-transfer limitations become more of a concern (decreasing $k_m$), a large duty cycle or cathodic potential would favour the undesired reaction I $\rightarrow$ U more than the desired reaction A $\rightarrow$ I. Therefore, as expected and as the calculations have indicated,

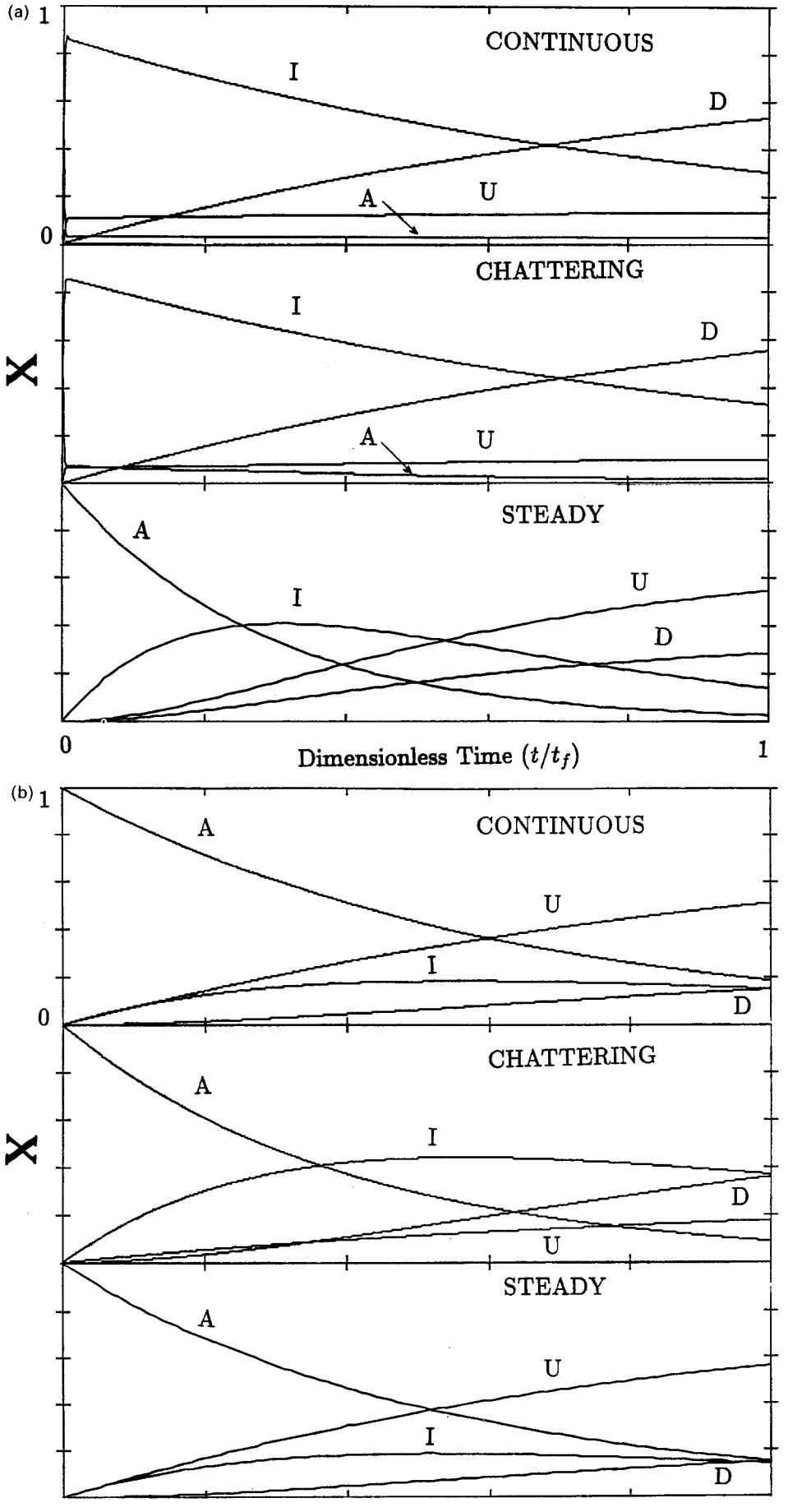


Fig. 7. The dimensionless concentration profiles $x$ over the batch period on applying the best steady potential, the best continuous, and optimal chattering potential controls for (a) low mass-transfer resistance, $k_m = 10^5\,\mathrm{cm\,h^{-1}}$, and (b) high mass-transfer resistance, $k_m = 1\,\mathrm{cm\,h^{-1}}$.

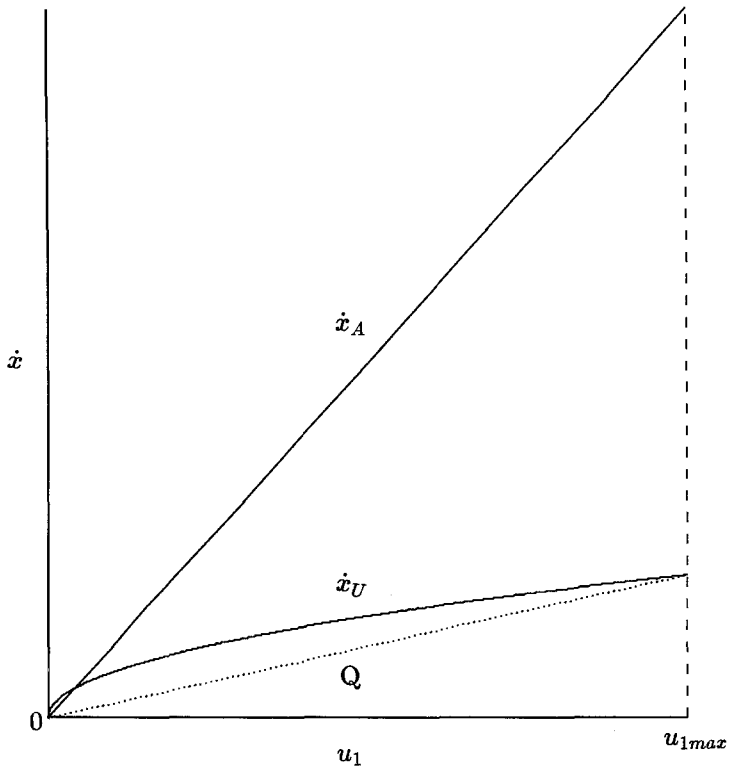


Fig. 8. Dependence of the reaction velocities given by Equations 38 and 41 on the control $u_1$ in the limit of no mass-transfer resistance. The set $\dot{x}_U$ is a nonconvex function of $u_1$, whereas the set $\dot{x}_A$ is convex. Any point, Q, on the dotted line represents a velocity $\dot{x}_U$ attained by perturbing $u_1$ between 0 and $u_{1\max}$ at an infinite frequency at some duty cycle $\theta$ (i.e. chattering control).

the duty cycle and the cathodic potential decrease with $k_m$ in the early portion of the reaction. At the largest mass-transfer resistance used ($k_m = 1\,\mathrm{cm\,h^{-1}}$), only a small amount of A can be converted to the intermediate during the early stage of the batch reaction. Therefore, the continuous potential and the duty cycle decrease slowly over the batch period so that intermediate is continually produced to maximize the production of the desired compound.

### 3.2. Comments

The use of chattering control to enhance product selectively is discussed in the chemical reaction-engineering literature. For example, Horn and Bailey [39] demonstrated that the selectivity of product $P_2$ for the heterogeneous reaction scheme given below increases under chattering concentration control of the reactant R

$$\begin{aligned} \mathrm{R} &\rightleftharpoons \mathrm{A} \\ \mathrm{R} + \mathrm{A} &\rightarrow 2\mathrm{P}_1 \\ \mathrm{R} &\rightarrow \mathrm{P}_2 \end{aligned} \tag{44}$$

where A is an adsorbed intermediate. They argued that selectivity enhancement is possible because the reaction velocities $\dot{x}$ are nonconvex functions of the concentration of the reactant R through the state equations $\dot{x} = f(x,u)$. Their development is based upon a result of Warga [32] who determined that if $f$ is analytic, then any trajectory $x(t)$ obtained from a velocity lying in the convex hull of $f(x,u)$ can be generated from a linear combination of the velocities that lie in $f(x,u)$, i.e. by using chattering control.

The solid lines on Fig. 8 illustrate the qualitative nature of the velocity sets (Equations 38 and 41) for the example E–C, E reaction scheme under kinetic-controlled conditions. The velocity set $\dot{x}_U$ of the undesired electrochemical reaction is seen to be nonconvex. Consequently, rapid perturbation of the control $u_1$ between 0 and $u_{1\max}$ at some duty cycle $\theta$ gives rise to an average reaction velocity, denoted by Q on the dotted line, which is always below the solid curve. From this simple geometric perspective, it is clear that a chattering control would result in a lower production of the undesired compound in comparison to steady control.

Because electrochemical-reaction rates typically show an exponential dependence on potential, the controls $u_i(\exp[-\alpha_i f E])$ form a nonconvex set for reactions with differing transfer coefficients $\alpha_i$. Based on this observation, a qualitative examination of the $u_i$ can determine whether a chattering potential control would be better than a continuous potential control. As an example, Fig. 9 shows the controls $u_1$ and $u_2$ which are directly related to rates of the desired (A → I) and the undesired (I → U) electrochemical reactions $r_{AI}$ and $r_{IU}$, respectively, for the reaction sequence of Fig. 1. The cathodic potential increases from its anodic limit (lower left portion), where reactions occur under kinetic-controlled conditions, to the cathodic limit (upper right portion), where the reactions may occur under mass-transfer controlled conditions. The case where the desired reaction is more sensitive to electrode potential ($\alpha_1 > \alpha_2$) and the opposite situation ($\alpha_1 < \alpha_2$) are both sketched, lower and upper solid curves, respectively. As the steady potential increases cathodically from the anodic limit, the ratio $r_{AI}/r_{IU}$ goes through a maximum if $\alpha_1 > \alpha_2$ since $r_{AI}$ increases faster with potential than $r_{IU}$ in the kinetic-controlled regime while the opposite occurs in the mass-transfer influ-

enced regime. Suppose the control $u_1$ corresponding to this best steady potential is $u_{1fix}$. The figure clearly shows that a chattering control switching between O and P with $u_{1avg} = u_{1fix}$ has an associated $u_{2avg}$ (point T), which is less than $u_2$ of a steady potential for $\alpha_1 > \alpha_2$ (point R), and greater than $u_2$ of a steady potential for $\alpha_1 < \alpha_2$ (point S). Hence, a chattering potential control would increase $r_{AI}/r_{IU}$ and reaction selectivity for $\alpha_1 > \alpha_2$ and decrease $r_{AI}/r_{IU}$ and reaction selectivity for $\alpha_1 < \alpha_2$ relative to a steady potential control. Fedkiw and Scott [40] determined heuristically for the E–C, E reaction scheme (among others) that for $\alpha_1 > \alpha_2$ a chattering potential control results in a greater differential selectivity at a fixed production rate of the desired product D compared to the best steady control and vice versa for $\alpha_1 < \alpha_2$. This present work is a confirmation of these earlier results.

The simple qualitative analysis described above can be carried out for other reaction sequences to determine whether a chattering potential control might lead to an improved reactor performance. If a chattering control is optimal, then the resulting functional can be maximized by directly computing appropriate $\theta^k$ and $u^k$ (Equation 25), an approach we expand upon in a separate communication [37].

## 4. Summary

Optimal-control theory was applied to calculate the time-varying electrode potential which maximizes the concentration of the desired product, D, at the end of a batch electrochemical reaction (Fig. 1). Chattering potential control was optimal if the transfer coefficient of the first reaction is greater than that of the second. A continuous potential control is optimal in the reverse case. The physical model for the reactor is fairly simple. Hence, the analysis by no means predicts the control strategy that should actually be implemented. However, the simplified perspective allows rapid computation, as compared to a more elaborate physical model, to provide a quick estimate of the improvements which could result on applying an optimal time-varying potential.

## Acknowledgement

This work was supported, in part, by the National Science Foundation under grant CPE 8414166. The authors thank Prof. Joseph C. Dunn for stimulating discussions on optimal control.

## References

[1] G. P. Sakellaropoulous, *AIChE J.* **25**(5) (1979) 781.

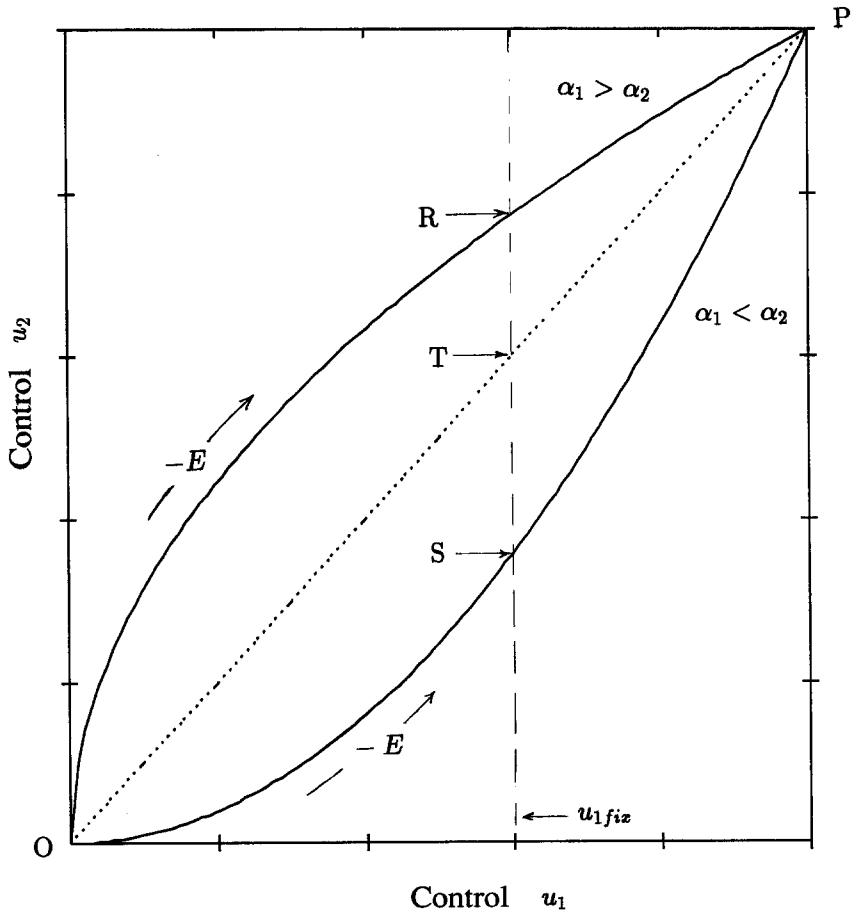


Fig. 9. The effect of chattering potential on the controls $u_1$ and $u_2$ which are directly related to the desirable and undesirable reaction rates, respectively. For a fixed $u_1$ given by $u_{1fix}$, the associated control $u_2$ under steady potential is given by R and S, for $\alpha_1 > \alpha_2$ and $\alpha_1 < \alpha_2$, respectively, for the example E–C, E reaction sequence. For a chattering potential control switching between O and P such that $u_{1avg} = u_{1fix}$, the associated $u_{2avg}$ is given by T.

[2] G. P. Sakellaropoulous and G. A. Francis, *J. Electrochem. Soc.* **126** (1979) 1728.
[3] F. J. M. Horn and R. C. Lin, *I & EC Proc. Des. Devel.* **6** (1967) 21.
[4] F. A. Fine and S. G. Bankoff, *I & EC Fundamentals* **6** (1967) 293.
[5] L. Padmanabhan and S. G. Bankoff, *Automatica* **8** (1972) 65.
[6] D. L. Schwieg and T. Z. Fahidy, *Int. J. Control* **20** (1974) 811.
[7] M. A. Latifi, S. Risson and A. Storck, *Entropie* **163** (1991) 37.
[8] A. J. Avila and M. J. Brown, *Plating* **57** (1970) 1105.
[9] H. Y. Cheh, *J. Electrochem. Soc.* **118** (1971) 551.
[10] D. T. Chin, *ibid.* **130** (1983) 1657.
[11] J. Cl. Puippe and F. Leaman (eds), 'Theory and Practise of Pulse Plating', AESF (1986).
[12] T. R. Nolen and P. S. Fedkiw, *J. Appl. Electrochem.* **20** (1990) 370.
[13] R. Bakshi, Ph.D. Thesis, North Carolina State University, Raleigh, NC (1992).
[14] W. H. Ray, 'Advanced Process Control', McGraw Hill, New York (1981).
[15] M. Athans and P. L. Falb, 'Optimal Control', McGraw Hill, New York (1966).
[16] M. M. Denn, 'Optimization by Variational Methods', McGraw Hill, New York (1969).
[17] Iu. P. Petrov, 'Variational Methods in Optimal Control Theory', Academic Press, New York (1968).
[18] S. K. Mitter, *Automatica* **3** (1967) 135.
[19] C. W. Merriam, *Information and Control* **8** (1965) 215.
[20] L. S. Pontryagin, 'The Mathematical Theory of Optimum Processes', Wiley Interscience, New York (1962).
[21] L. T. Biegler, *Comput. & Chem. Eng.* **8** (1984) 243.
[22] T. H. Tsang, D. M. Himmelblau and T. F. Edgar, *Int. J. Control* **21**(5) (1975) 763.
[23] C. P. Neuman and A. Sen, *Automatica* **9** (1973) 601.
[24] C. P. Neuman and A. Sen, *IEEE Trans. Autom. Control.* **19** (1974) 67.
[25] M. Minoux, 'Mathematical Programming', Wiley-Interscience, New York (1986).
[26] J. C. Dunn, *Control Dyn. Syst.* **29**(2) (1988) 135.
[27] D. G. Luenberger, 'Optimization by Vector Space Methods', John Wiley, New York (1969).
[28] L. Hasdorff, 'Gradient Optimization and Nonlinear Control', John Wiley, New York (1976).
[29] L. Armijo, *Pac. J. Math.* **16** (1966) 1.
[30] V. F. Demyanov and A. M. Rubinov, 'Approximate Methods in Optimization Problems', American Elsevier, New York (1970).
[31] D. Bertsekas, *IEEE Trans. Autom. Control* **21** (1976) 174.
[32] J. Warga, *J. Math. Anal. Appl.* **4** (1962) 11.
[33] M. Fjeld, *Chem. Eng. Sci.* **29** (1974) 921.
[34] R. V. Gamkrelidze, 'Principles of Optimal Control Theory', Plenum Press, New York (1978).
[35] J. C. Smeltzer and P. S. Fedkiw, *J. Electrochem. Soc.* **139** (1992) 1358.
[36] R. T. Rockafellar, 'Convex Analysis', Princeton University Press, Princeton, NJ (1970).
[37] R. Bakshi and P. S. Fedkiw, 'The Optimal Time-Varying Cell-Voltage Control for a Parallel-Plate Reactor', under review (1993).
[38] J. C. Puippe and N. Ibl, *J. Appl. Electrochem.* **10** (1980) 775.
[39] F. J. M. Horn and J. E. Bailey, *J. Optimization Theory Appl.* **2** (1968) 441.
[40] P. S. Fedkiw and W. D. Scott, *J. Electrochem. Soc.* **131** (1984) 1304.